

# Novel elastic material from collagen for tissue engineering

Shunji Yunoki · Kazuo Mori · Takeshi Suzuki ·  
Nobuhiro Nagai · Masanobu Munekata

Received: 12 April 2005 / Accepted: 8 March 2006 / Published online: 3 February 2007  
© Springer Science+Business Media, LLC 2007

**Abstract** Elastic collagen gel (*e*-gel) was prepared from salmon atelocollagen fibrillar gel reinforced by 1-ethyl-3-(3-dimethylaminopropyl)-carbodiimide (EDC) mediated cross-linking (*f*-gel). The preparation consisted of a simple heat treatment of the *f*-gel at 80 °C, in which the *f*-gel drastically shrank and the collagen fibril structure was deformed. The *e*-gel obtained showed rubber-like elasticity; its stress–strain behavior little changed through repeated stretching. The elongation at the breaking point was approximately 230%. Furthermore, normal human osteoblasts showed good attachment and proliferation on the *e*-gel. These results suggest its potential to be utilized for the development of tissue engineering.

## Introduction

Tissue engineering is a field of research which aims at regenerating tissues and organs. Tissues are basically made up of cells and extracellular matrix. A major goal of tissue engineering is the preparation of a suitable scaffold to integrate tissues/organs as well as for cells to

proliferate, migrate and differentiate into environmental tissues/organs.

Type I collagen (abbreviated as collagen) is an extracellular matrix protein that is widely used as a scaffold material for tissue engineering, for which various forms of collagen such as fiber, gel, or sponge-like matrix have been utilized. Collagen fibers for artificial ligament have been fabricated by the extrusion of collagen dispersion to fiber formation buffer [1, 2]. Collagen molecules self-assemble and form fibrils under physiological conditions [3–5]. Networks of collagen fibrils create a matrix gel, which has been used for 3-D cellular matrices for the tissue engineering of cartilage [6, 7]. Lyophilized collagen sponges from collagen solution have been the most studied tissue engineering materials; these sponges have been used for artificial skin [8, 9], liver [10], and cartilage [11–13]. However, the mechanical properties of the collagen materials that have previously been developed are far different from the actual tissues, especially in their elasticity. Most collagen materials become brittle and fail under quite low strains, which limits their application to tissue engineering materials.

Recently, we developed collagen fibrillar gel as a scaffold prepared from low-denaturation temperature salmon collagen by the introduction of 1-ethyl-3-(3-dimethylaminopropyl)-carbodiimide (EDC) mediated cross-linking among collagen fibrils during its fibril formation [14]. A human cell showed good proliferation on the gel rather than on the porcine collagen gel. Although common collagen materials dissolved in water at a temperature above their denaturation temperature, we found that the EDC cross-linked salmon collagen gel drastically shrank at a high temperature without remarkable dissolution. The

---

S. Yunoki (✉) · N. Nagai · M. Munekata  
Division of Molecular Chemistry, Graduate School of  
Engineering, Hokkaido University, Kita-13, Nishi-8,  
Kita-ku, Sapporo, Hokkaido 060-8628, Japan  
e-mail: yunoki@cris.hokudai.ac.jp

K. Mori · T. Suzuki  
Ihara & Company Ltd., 3-263-23 Zenibako, Otaru,  
Hokkaido 047-0261, Japan

collagen gel obtained interestingly showed rubber-like elasticity and high stretchability. Here, we report on the preparation of the elastic collagen materials and their mechanical/biological properties.

## Materials and methods

### Preparation of cross-linked fibrillar collagen gel (*f*-gel)

Salmon atelocollagen (SC) was prepared from the fresh skin of chum salmon (*Oncorhynchus Keta*) by acid solubilization and subsequent pepsin digestion [14]. The introduction of EDC (Dojindo, Tokyo) mediating cross-linking during the fibril formation of SC was performed by a mixture of acidic SC solution and EDC solution in pH 6.8, 30-mM Na-phosphate buffer including 70 mM NaCl, according to our previous report [14]. EDC was dissolved in the buffer to a concentration of 100 mM. The EDC solution (40 ml) was added to an equal volume of the acidic SC solution at 4 °C with stirring. The mixture was immediately poured into plastic petri dishes (diameter of 100 mm) to a depth of 10 mm. Following incubation at 4 °C for 24 h, fibrillar gel was provided at final EDC concentration of 50 mM (*f*-gel).

### Preparation of elastic collagen gel (*e*-gel)

The elastic collagen gel (*e*-gel) was prepared from the *f*-gel by heat treatment. The *f*-gel in the plastic petri dish was soaked in water at 80 °C, and then gradually shrunk. After 10-min soaking, circular *e*-gel (thickness: 3.1 mm, diameter: 25 mm) was obtained. The loss of collagen was calculated from the decrease in the weight of the collagen ( $n = 3$ ), as follows;

$$\text{Loss of collagen (wt. \%)} = (W_e - W_f)/W_f \times 100$$

where  $W_e$  and  $W_f$  are the dry weight of the *e*-gel and collagen solution used to prepare the *f*-gel, respectively.

### Microscopic observation

The collagen fibrils were observed by high-resolution scanning electron microscopy (SEM; JSM-6500F, JEOL, Japan). The preparation of the specimen was performed according to a previous report [14]. Briefly, the gels were fixed by glutaraldehyde and then dehydrated by ethanol and subsequent isoamyl

acetate. The gels were subsequently subjected to a critical point drying. The dried gels were coated with Au using an ion coater (E-1010; Hitachi, Japan) and subjected to the SEM measurements. The SEM apparatus was operated at 5.0 kV and a magnification of 15,000.

### Mechanical tests

Tensile mechanical tests were carried on the *e*-gel using a texture analyzer (model TA-XT2i; Stable Micro Systems, U.K.). The *e*-gel was cut into rectangular specimens ( $5 \times 3.1 \times 12$  mm) using a razor blade, and both ends of the specimens were gripped to achieve a gauge length of 8 mm. Strains (the change in length divided by the initial length) were calculated using crosshead displacement; stresses were calculated by dividing the force data by the cross-sectional area of the specimens (assumed to remain constant). All specimens were kept hydrated with water before the tests were initiated. The following data were collected: (A) stress–strain curve to the breaking point, (B) stress–relaxation, and (C) hysteresis loops. The experimental conditions were as follows:

- (A) Stress–strain curve to the breaking point: stress–strain curves were determined by a tensile test in a strain rate of 0.1 mm/s to the breaking point, and the elongation at break was determined ( $n = 7$ ).
- (B) Stress–relaxation: three types of experimental conditions were employed for elongation of the specimens.

*Condition-1:* the specimens were loaded at a strain rate of 0.1 mm/s to achieve a strain of 8 mm (100% strain)

*Condition-2:* loaded at the at a strain rate of 0.1 mm/s to achieve a strain of 12 mm (150% strain)

*Condition-3:* loaded at the at a strain rate of 1 mm/s to achieve a strain of 8 mm (100% strain)

After the elongation, the strain was held for 120 s and the fall in stress was recorded ( $n = 7$ ). The stress–relaxation data were normalized for differences in the strain-induced stress by expressing each trial as a fraction of the maximum (i.e. initial) value.

- (C) Hysteresis loops: hysteresis loops were obtained by repeated cyclical loading using the three types of elongation conditions. These cycles were repeated 10 times ( $n = 5$ ).

## Cell culture

Normal human osteoblasts (Asahi Techno Glass, Japan) were cultured in Osteoblast Growth Medium (Asahi Techno Glass, Japan) at 310 K in air containing 5% CO<sub>2</sub> ( $n = 3$ ). The culture medium was changed every 3 days. At semi-confluence, the cells were subcultured in the same medium. The cells before passage 6 were used for the SEM observation. The cells were seeded on the *e*-gel at a density of  $1 \times 10^4$  cells cm<sup>-2</sup>. After 2 days of cultivation, the morphology of the cells attached on the *e*-gel were observed by SEM at a magnification of 500 and 2000, according to the method described above.

## Results

### Preparation of *e*-gel

The mixture of the acidic SC solution and neutral Na-phosphate buffer including EDC caused the introduction of EDC cross-linking during fibril formation [14]. The obtained *f*-gel was semitransparent, as shown in Fig. 1a. After the heat treatment at 80 °C, the *f*-gel shrunk drastically (diameter; 100–25 mm, thickness; 10–3.1 mm) and formed *e*-gel, which was white and opaque, as shown in Fig. 1b. The loss of collagen through the above procedure was estimated to be  $17.1 \pm 1.0$  (mean  $\pm$  SD;  $n = 3$ ) wt.%.

### Deformation of fibril structure

The fibril structures on the *f*-gel and *e*-gel were observed by SEM (Fig. 2). Figure 2a shows the well-developed networks of nano-fibrils on the *f*-gel, as previously reported [14]. The width of the fibrils was in the range of 50–100 nm. However, a wider (width;

>400 nm) and winding fibril-like structure was observed on the *e*-gel (Fig. 2b), indicating that the fibril structure of collagen was deformed through the heat treatment.

### Mechanical properties

The mechanical properties of the *e*-gel were evaluated by tensile tests. The *f*-gel rarely had elasticity and stretchability similar to the usual collagen materials (data not shown). However, the *e*-gel showed rubber-like elasticity and high stretchability. Figure 3 shows the representative stress–strain curve to the breaking point obtained in the strain rate of 0.1 mm/s (i.e. 1.25%/s). The mean values  $\pm$  SD of ultimate tensile strength and elongation at the break of the *e*-gel were  $19.4 \pm 4.9$  kPa and  $225 \pm 31\%$ , respectively ( $n = 7$ ). At the early stage of loading ( $\sim 100\%$  strain), stress was almost linearly increased depending on the strain. Above a strain of 100%, an increase in strain hardening was observed.

Figure 4a shows the stress–relaxation behavior expressed as the measured stresses. When the stress was detected after loading of *condition-1* (100% strain; 1.25%/s strain rate), the initial stress of  $6.48 \pm 1.58$  kPa was decreased to  $5.24 \pm 1.33$  kPa (means  $\pm$  SD;  $n = 7$ ). The stress–relaxation curve obtained by using *condition-3* was similar to that using *condition-1*; however, the stresses were significantly increased with an increase in the strain (100–150%; *condition-2*).

When the stresses developed by each specimen were normalized over time by expressing them as a fraction of their maximum (i.e. initial) stress, the resulting stress–relaxation curves after loading were changed depending on both strain and strain rates (Fig. 4b). The normalized stress–relaxation after loading under *condition-1* was determined to be  $13.7 \pm 1.2\%$  (means  $\pm$  SD;  $n = 7$ ), and showed a tendency to be increased by increase in strain (100–150%; *condition-*

**Fig. 1** Appearance of (a) *f*-gel and (b) *e*-gel

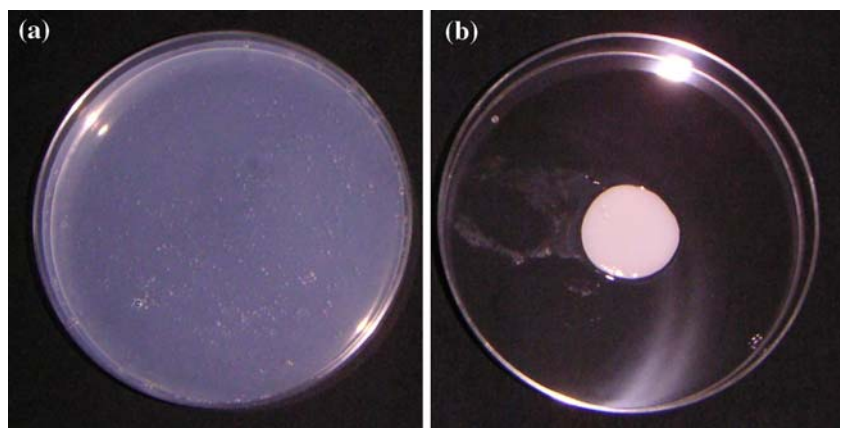


**Fig. 2** Scanning electron microscopy images of (a) *f*-gel and (b) *e*-gel. Original magnification  $\times 15,000$

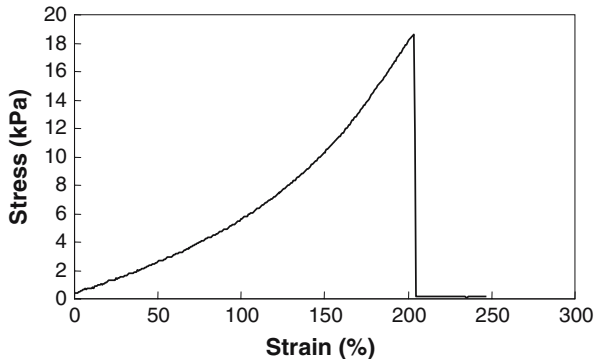
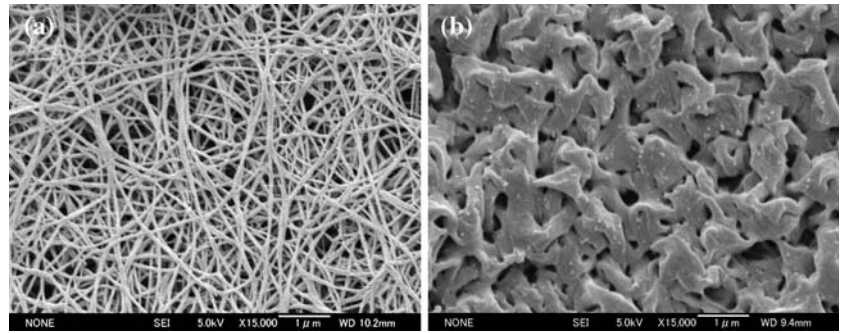


**Fig. 3** Representative stress–strain curve generated from tensile testing of *e*-gel. The specimen ( $5 \times 3.1 \times 12$  mm) was gripped to achieve a gauge length of 8 mm and stretched in the strain rate of  $1.25\%/s$

2). That after loading under *condition-3* was significantly higher than that under *condition-1* (Fig. 4b). At 120 s-hold of strain, the decreases of the stresses were  $16.8 \pm 3.1\%$  and  $18.6 \pm 1.7\%$  (means  $\pm$  SD;  $n = 7$ ) under *condition-2* and *-3*, respectively, against the maximum values.

Figure 5 shows the hysteresis loops obtained by the 10-times repeated cyclical loading performed under the three types of elongation conditions. In the strains,

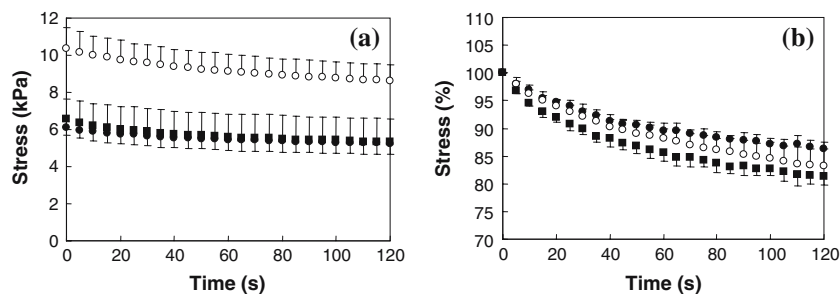


**Fig. 4** Stress–relaxation curves of *e*-gel (a) expressed as the measured stresses and (b) normalized over time by expressing them as a fraction of their maximum (i.e. initial) stress. The specimens ( $5 \times 3.1 \times 12$  mm) were loaded to a certain strain, and then held at that strain for 120 s as the fall in stress was recorded. Closed circles, loaded at a strain rate of  $1.25\%/s$  to achieve a

almost linear stress–strain behavior was obtained as described above. Here, the *e*-gel can be seen to exhibit almost fully repeatable stress–strain curves. Similar results were repeatedly obtained by the each five tests using the three types of elongation conditions. Only the stresses obtained in the first elongation (the arrows in Fig. 5) was slightly higher than those in the latter cycles. At the same time, slight minus values of stress at the zero position were observed, indicating the slight deflection of the specimen.

#### Cell morphology

The cell morphology of human osteoblasts was studied on the *e*-gel after 2 days of culturing. The cells appeared elongated, flat and intimately attached to the surface of the *e*-gel (Fig. 6). About one-half of the surface was filled with the cells, according to the SEM observation.

#### Discussion

In this study we prepared elastic collagen gel from EDC cross-linked salmon collagen fibrillar gel by heat treatment, and evaluated the structural, mechanical,

strain of 100% (*condition-1*); open circles, loaded at a strain rate of  $1.25\%/s$  to achieve a strain of 150% (*condition-2*); closed squares, loaded at a strain rate of  $12.5\%/s$  to achieve a strain of 100% (*condition-3*). The values are expressed as means  $\pm$  SD ( $n = 7$ )

**Fig. 5** Representative loading-de-loading cycles (hystereses) for a specimen ( $5 \times 3.1 \times 12$  mm) of *e*-gel converted to stress-strain relationships. The specimen was loaded and de-loaded cyclically using (a) a strain rate of 1.25%/s in a strain ranged from 0 to 100% (*condition-1*), (b) a strain rate of 1.25%/s in a strain ranged from 0 to 150% (*condition-2*), and (c) a strain rate of 12.5%/s in a strain ranged from 0 to 100% (*condition-3*). These cycles were repeated 10 times. The arrow indicates the stress-strain curve of the first stretching

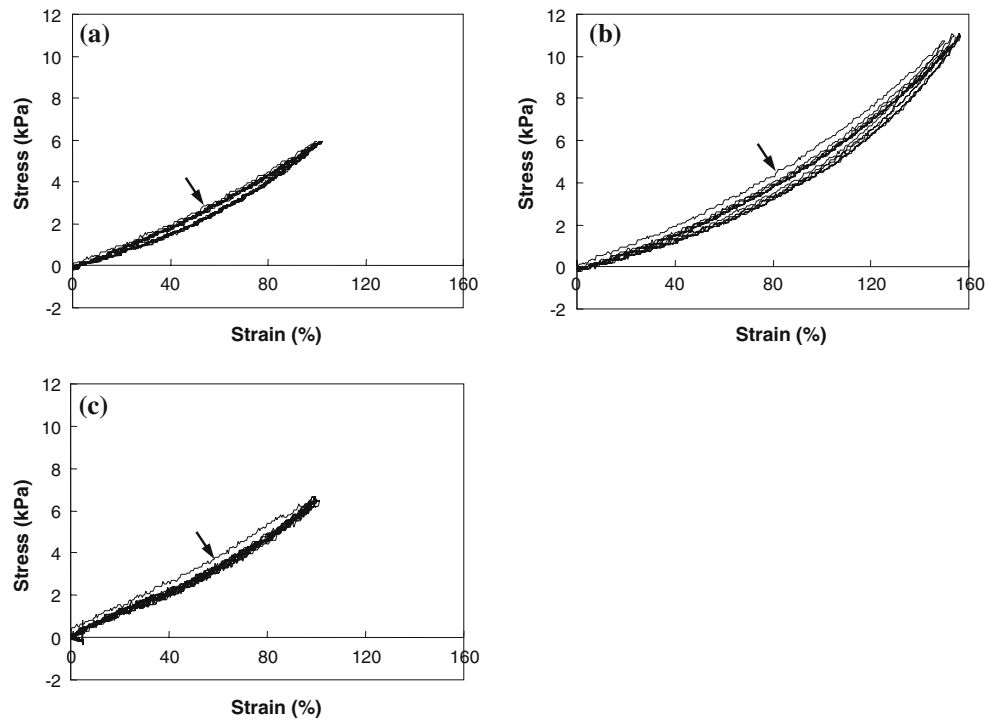
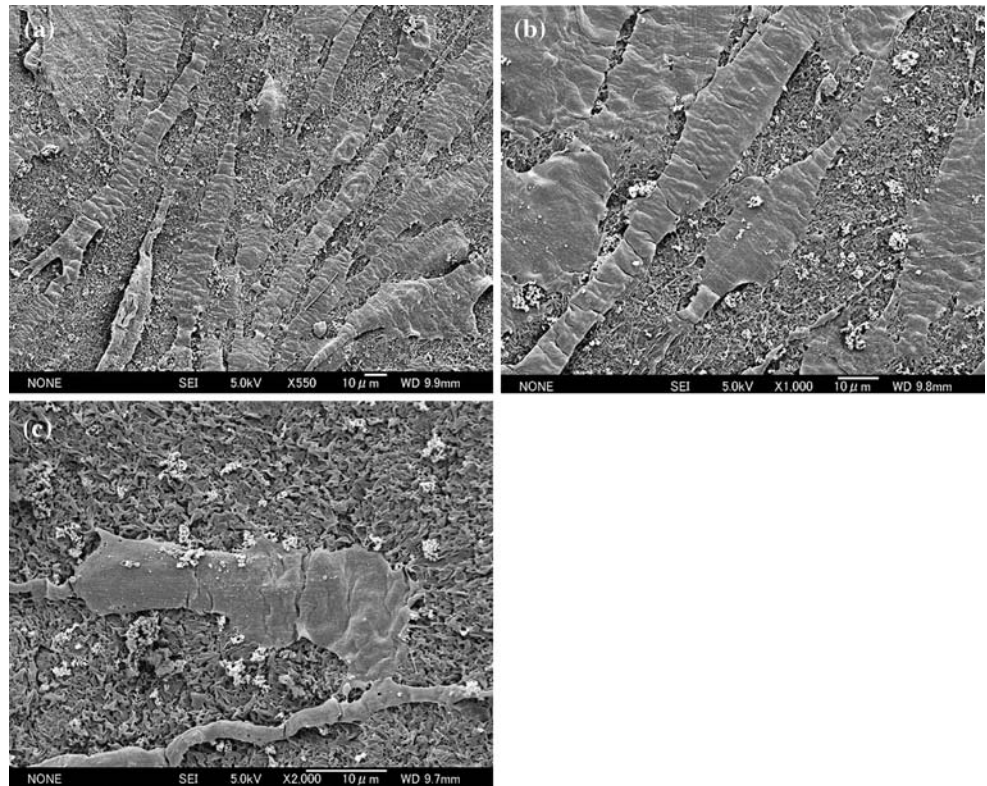


**Fig. 6** Scanning electron microscopy images of human osteoblasts on *e*-gel after 2 days of culturing. Original magnifications (a)  $\times 550$ , (b)  $\times 1000$ , and (c)  $\times 2000$



and biological properties. Those investigations showed that *e*-gel is a novel collagen material with rubber-like elasticity and high stretchability with potential to be utilized as a tissue engineering material.

Drastic shrinkage of the *f*-gel, the starting material of the *e*-gel, occurred through the heat treatment. The low loss of collagen (only 17.1%) through the heat treatment at such a high temperature indicates that the

cross-linkage among the collagen molecules and fibrils was uniformly introduced. However, rod-like triple-helical collagen molecules certainly denatured to the random-coil form (gelatin). The drastic shrinkage of the *f*-gel and structural deformation can be explained by the denaturation. The wide and winding fibril-like structure of the *e*-gel should be directly derived from the collagen nano-fibrils of the *f*-gel through swelling of the fibrils by comparison of both surface structures.

The stress–strain curve demonstrated high stretchability of the *e*-gel. According to the report by Koide and Daito [15], collagen films reinforced by traditional cross-linking reagents, glutaraldehyde and tannic acid, showed only small elongation at the breaking point (6.6% and 12.4%, respectively). Weadock et al. [16] showed small ultimate strains (approximately 40% and 30%) of collagen fibers cross-linked by UV irradiation and dehydrothermal treatment, respectively. Even a purified skin with an intact fibrous collagen network gives elongation at a breaking point of 125% [16]. Recently, it was reported that a chemically cross-linked collagen-elastin-glycosaminoglycan scaffold, which are the

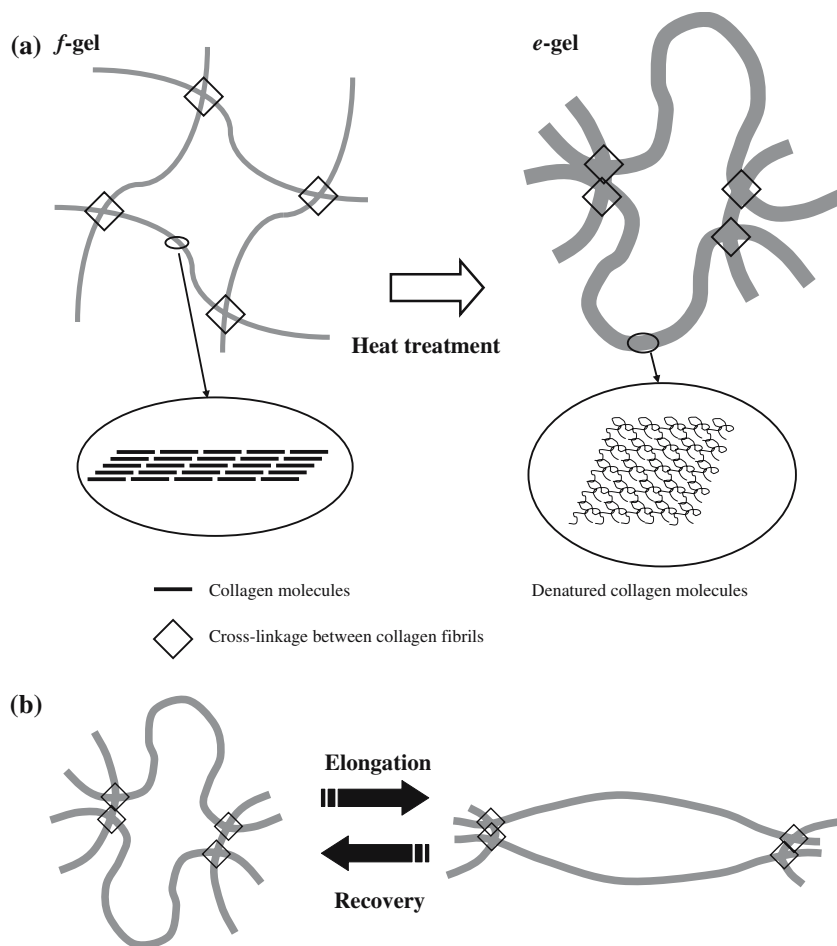
contents analogous to the actual tissue/organs, demonstrated good stretchability (150% strain) [17]. To the best of our knowledge, this is the first report of a material from collagen with elongation at a breaking point over 200%.

Although the mechanism of the high stretchability was not well understood, the denaturation of the collagen molecules probably plays an important role in the elongation, i.e., the bend structure of denatured collagen fibrils is considered to provide its rubber-like stretchability. The detailed mechanism involved in this will be discussed below.

Stress–relaxation tests under constant strains are useful for assessing plastic deformation. The stress–relaxation behavior indicates that the *e*-gel was not fully elastic, i.e., a viscoelastic material. The strain- and strain rate-dependence of stress–relaxation indicates that the *e*-gel had viscosity as well as elasticity.

Cross-linked rubbers show complete repeatability of the stress–strain curves obtained by a repeated cyclical loading. The *e*-gel exhibited almost the same stress–strain curves in the range of strain from 0 to 100%. The slight plastic deformation during and after stretching

**Fig. 7** Schematic drawing of (a) considerable structural change from *f*-gel to *e*-gel, and (b) that obtained through stretching



could be occurring predominantly on the first cycle, resulting in good repeatability in the latter cycles. The plastic deformation is probably due to the destruction of collagen fibrils with relatively low strength. The repeatability of the stress–strain behavior in such a high strain (100%) appears to be fairly uncommon in the materials from biopolymers.

Figure 7 shows a schematic drawing of the considerable structural change from *f*-gel to *e*-gel, and that obtained through stretching. We think the mechanism of rubber-like elasticity and high stretchability works as follows: upon preparation of the *f*-gel, the cross-linking derived from EDC is introduced among the collagen molecules and fibrils. By heat treatment, the cross-linked collagen fibrils shrink, maintaining the cross-linkage among the collagen molecules and fibrils through the denaturation of triple-helical collagen molecules to the random-coil form (Fig. 7a). At the same time, uncross-linked collagen molecules and fibrils are lost through dissolution to water. The interesting mechanical properties of the *e*-gel are probably due to the bend fibrils being interconnected by cross-linkage (Fig. 7b).

EDC cross-links collagen molecules by the formation of isopeptides without being incorporated itself, thus precluding depolymerization and the possible release of potentially cytotoxic reagents. Furthermore, the by-product of the cross-linking reaction and un-reacted EDC in the *f*-gel should be completely removed by the drastic shrinkage in hot water. It is expected that the *e*-gel has good biocompatibility and no cytotoxicity.

Intimate attachment and active proliferation of human cells was observed on the *e*-gel, suggesting the potential of this rubber-like material for tissue engineering. The denaturation of collagen molecules contributed to cellular responses such as cell attachment and proliferation [8], but lowered their biological stability, because the random-coil structure became more susceptible to proteolytic enzymes than the triple-helix structure of collagen [18]. When *e*-gel is used for tissue engineering materials that require long-term maintenance in vivo, further cross-linking is needed.

In conclusion, we successfully fabricated an elastic collagen material from EDC cross-linked SC fibrillar gel by heat treatment. The elastic collagen demonstrated

rubber-like mechanical properties which have not yet been reported in collagen-based biomaterials. The human cells used here showed good attachment and proliferation on this elastic material, suggesting its potential to be utilized in the development of tissue engineering.

**Acknowledgements** Authors thank Dr. T. Sakurai for his helpful advice on the mechanical tests.

## References

1. K. S. WEADOCK, E. J. MILLER, L. D. BELLINCAMPI, J. P. ZAWADSKY, M. G. DUNN, *J. Biomed. Mater. Res.* **29** (1995) 1373
2. K. S. WEADOCK, E. J. MILLER, E. L. KEUFFEL, M. G. DUNN, *J. Biomed. Mater. Res.* **32** (1996) 221
3. J. GROSS, D. KIRK, *J. Biol. Chem.* **233** (1958) 355
4. B. R. WILLIAMS, R. A. GELMAN, D. C. POPPKE, K. A. PIEZ, *J. Biol. Chem.* **253** (1978) 6578
5. D. L. HELSETH Jr., A. VEIS, *J. Biol. Chem.* **256** (1981) 7118
6. K. KATSUBE, M. OCHI, Y. UCHIO, S. MANIWA, M. MATSUSAKI, M. TOBITA, J. IWASA, *Arch. Orthop. Trauma Surg.* **120** (2000) 121
7. M. OCHI, Y. UCHIO, M. TOBITA, M. KURIWAKA, *Artif. Organs* **25** (2001) 172
8. M. KOIDE, K. OSAKI, J. KONISHI, K. OYAMADA, T. KATAKURA, A. TAKAHASHI, K. YOSHIZATO, *J. Biomed. Mater. Res.* **27** (1993) 79
9. B. HAFEMANN, K. GHOFRANI, H. G. GATTNER, H. STIEVE, N. PALLUA, *J. Mater. Sci.: Mater. Med.* **12** (2001) 437
10. X. H. WANG, D. P. LI, W. J. WANG, Q. L. FENG, F. Z. CUI, Y. X. XU, X. H. SONG, M. VAN DER WERF, *Biomaterials* **24** (2003) 3213
11. M. HOLMES, R. G. VOLZ, M. CHVAPIL, *Surg. Forum* **26** (1975) 511
12. K. MATSUDA, N. NAGASAWA, S. SUZUKI, N. ISSHIKI, Y. IKADA, *J. Biomater. Sci. Polym. Ed.* **7** (1995) 221
13. S. MIZUNO, F. ALLEMANN, J. GLOWACKI, *J. Biomed. Mater. Res.* **56** (2001) 368
14. S. YUNOKI, N. NAGAI, T. SUZUKI, M. MUNEKATA, *J. Biosci. Bioeng.* **98** (2004) 40
15. T. KOIDE, M. DAITO, *Dental Mat. J.* **16** (1997) 1
16. L.H. H. OLDE DAMINK P. J. DIJKSTRA, M. J. A. VAN LUYN, P. B. VAN WACHEM, P. NIEUWENHUIS, J. FEIJEN, *J. Mater. Sci. Mater. Med.* **6** (1995) 460
17. W. F. DAAMEN, H. T. VAN MOERKERK, T. HAFMANS, L. BUTTAFOCO, A. A. POOT, J. H. VEERKAMP, T. H. VAN KUPPEVELT, *Biomaterials* **24** (2003) 4001
18. S. D. GORHAM, N. D. LIGHT, A. M. DIAMOND, M. J. WILLINS, A. J. BAILEY, T. J. WESS, N. J. LESLIE, *Int. J. Biol. Macromol.* **14** (1992) 129